Dissecting the role of the elongation factor 1A isoforms in hepatocellular carcinoma cells by liposome-mediated delivery of siRNAs

Rossella Farra[a], Bruna Scaggiante[b], Chiara Guerra[b], Gabriele Pozzato[c], Mario Grassi[a], Fabrizio Zanconati[c], Francesca Perrone[b], Cinzia Ferrari[d], Francesco Trotta[d,e], Gabriele Grassi[b,*], Barbara Dapas[b]

[a] *Department of Industrial Engineering and Information Technology, University of Trieste, Italy*
[b] *Department of Life Sciences, University of Trieste, Italy*
[c] *Department of Medical, Surgery and Health Sciences, University of Trieste, Cattinara Hospital, Italy*
[d] *Department of Clinic-Surgical Sciences, Experimental Surgery Laboratory, University of Pavia, Italy*
[e] *U.O. di Chirurgia Generale e Toracica, Ospedale Maggiore, Lodi, Italy*

A R T I C L E   I N F O

A B S T R A C T

Eukaryotic elongation factor 1A (eEF1A), a protein involved in protein synthesis, has two major isoforms, eEF1A1 and eEF1A2. Despite the evidences of their involvement in hepatocellular carcinoma (HCC), the quantitative contribution of each of the two isoforms to the disease is unknown.

We depleted the two isoforms by means of siRNAs and studied the effects in three different HCC cell lines. Particular care was dedicated to select siRNAs able to target each of the two isoform without affecting the other one. This is not a trivial aspect due to the high sequence homology between eEF1A1 and eEF1A2.

The selected siRNAs can specifically deplete either eEF1A1 or eEF1A2. This, in turn, results in an impairment of cell vitality, growth and arrest in the G1/G0 phase of the cell cycle. Notably, these effects are quantitatively superior following eEF1A1 than eEF1A2 depletion. Moreover, functional tests revealed that the G1/G0 block induced by eEF1A1 depletion depends on the down-regulation of the transcription factor E2F1, a known player in HCC.

In conclusion, our data indicate that the independent targeting of the two eEF1A isoforms is effective in reducing HCC cell growth and that eEF1A1 depletion may result in a more evident effect.

1. Introduction

Hepatocellular carcinoma (HCC) is the predominant form of primary liver cancer and a leading cause of cancer-associated mortality worldwide. The high incidence of morbidity and mortality in HCC is predominantly attributed to late diagnosis (Ferlay et al., 2015; Jemal et al., 2011) of the disease and to the limited efficacy of currently available therapeutic approaches. Moreover, systemic chemotherapy is poorly effective due to the general HCC resistance to anticancer agents (Azmi et al., 2015).

Together these considerations clearly indicate that the development of novel therapeutic strategies for HCC are urgently required.

With the aim to identify novel biological targets to fight HCC, in this work, we continue our studies aimed at the definition of the role of eukaryotic elongation factor 1A (eEF1A) in HCC. eEF1A, a protein involved in the elongation step of protein synthesis (Scaggiante et al., 2014), has two major isoforms, eEF1A1 and eEF1A2. Whereas eEF1A1 is ubiquitously expressed, eEF1A2 expression is mostly confined to skeletal muscle, heart and nervous system. Beside the role in translation, defined as the "canonical function" of eEF1As, both isoforms possess "non-canonical functions" relevant for many cellular process such as cell cycle and apoptosis (Lamberti et al., 2004). Moreover, both eEF1A isoforms play a role in solid and hematologic human tumors, mainly due to the dysregulation of their non-canonical functions (Abbas et al., 2015).

We reported that in human HCC cell lines, eEF1A2 is overexpressed and that this overexpression correlates with cancer cell growth and differentiation phenotype (Grassi et al., 2007). Moreover, eEF1A2 overexpression has been detected in HCC human tumor specimens (Qiu et al., 2016; Schlaeger et al., 2008). Recently, it has been shown that eEF1A2 takes part in the eEF1A2/PI3K/AKT/mTOR-dependent stabilization of MDM4 (Mouse Double Minute homolog 4) which in turn inactivates the anti-oncogene p53 thus resulting in a pro-tumorigenic effect in HCC (Pellegrino et al., 2014). Notably, the activation of the EEF1A2/PI3K/AKT/mTOR/MDM4 axis significantly influences the survival probability of HCC patients. eEF1A2 has been also implicated in the oncogenic function of the mammalian timeless (TIM) protein in HCC (Elgohary et al., 2015). With regard to eEF1A1, we observed that its overexpression relates with HCC cell growth and differentiation phenotype (Grassi et al., 2007). Moreover, eEF1A1 seems to mediate the tumorigenic functions of the human HLA-F adjacent transcript 10 (FAT10) protein in HCC (Yu et al., 2012). Finally, we showed that the contemporary targeting of eEF1A1 and eEF1A2 by means of an aptameric DNA molecule resulted in the profound impairment of the viability of cultured HCC cell lines (Scaggiante et al., 2016).

Despite the above evidences of the eEF1A1 and eEF1A2 involvement in HCC, the quantitative contribution to HCC of each of the two isoform remains to be clarified. This aspect is relevant to determine their quantitative contribution to HCC and, in turn, which of the two isoforms is the most appropriate to target to fight HCC. Thus, in this work we have depleted each of the two isoforms by means of small interfering RNAs (siRNAs) and studied the effects in different HCC cell lines. Due to the high sequence homology between the two isoforms, 78% in the coding sequence and 92% in the amino acid sequence (Lund et al., 1996), particular care has been dedicated to select siRNAs able to specifically target one of the two isoforms leaving the level of the other almost unchanged.

2. Materials and methods

2.1. Cell cultures

The human HCC derived cell lines HuH7 and JHH6 were cultured as described (Farra et al., 2010, 2011) and assigned to medium and low hepatic differentiation grade on the base of the capacity to synthesize albumin and ferritin (Grassi et al., 2007), known markers of hepatic differentiation. The rat HCC derived cell line N1S1 was cultured in Dulbecco's modified Eagle's medium (DMEM) (Euroclone) containing 10%FBS, 100U/ml penicillin, 100ug/mL streptomycin and 2 mM L-glutamine (Euroclone).

2.2. siRNA transfection and uptake studies

The sequences of the anti eEF1A1 siRNA (siA1), the control siRNA (siGL2) and the anti E2F1 siRNA (siE2F1) were as described (Dapas et al., 2009; Lamberti et al., 2007). Their sequences are reported in Table 1 as well as the sequences of the two anti eEF1A2 siRNAs (siA2 and siA2bis).

The day before transfection, HCC cells were seeded at a density of 3.8×10^3 cells/cm^2 in 6 well microplate in the presence of 3 ml of complete medium. Transfections were performed either using the siGL2 labeled at the 5′ end of the sense strand by FITC (uptake studies), or the unlabeled siGL2 and the specific siRNAs (functional studies). Optimal transfection conditions were obtained by using Lipofectamine 2000 (1 mg/ml, Invitrogen) at a weight ratio siRNA-transfectant of 1:1 for all the cell lines used in this study. The mixture Liposome-siRNA (220 nM) was then administered to the cells for 3 h at 37 °C in the presence of serum-free medium Optimem (Invitrogen). Afterwards, transfection medium was removed, cells were washed with PBS and then 3 ml of PBS or complete medium were added to the cells, depending on whether cells were used for uptake or functional studies, respectively. For uptake studies, cells were trypsinized, re-suspended in 500 μl of PBS/BSA 0,5% and the number of fluorescein-positive cell was evaluated by flow cytometry (Cytomics FC500, Beckman Coulter).

2.3. Cell necrosis, viability, apoptoisis and cell cycle analysis

Cell viability, evaluated by MTT test, was performed as described (Baiz et al., 2009) seeding 4.0×10^3 cells of HuH7, JHH6 and N1S1 in 96 microplate. Cell necrosis was evaluated by lactate dehydrogenase (LDH) assay kit according to manufacturer instructions (BioVision Prod., Mountain View CA) as described (Baiz et al., 2009). Cell cycle analysis was performed as described (Farra et al., 2011). Briefly, twelve hours before harvesting, 70% confluent cells were pulsed with bromodeoxyuridine (BrdU) at a concentration of 10 μM. Cells were then prepared for BrdU staining as described (Grassi et al., 2005) except that resuspension in ice cold 70% ET-OH was protracted overnight, the treatment with 1 M HCl 0.5% BSA was prolonged to 1 h and incubation with fluorescein-isothiocyanate (FITC) – conjugated mouse monoclonal antibody (BD PharMigen) anti BrdU was extended to 1 h. Cells, resuspended in PBS containing 0.5% BSA, were analyzed by flow cytometry (FACScanto, Becton Dickinson) using the DIVA software.

Apoptosis, performed by annexin V test and PARP (Poly (ADP-ribose) polymerase) cleavage, were performed as previously described (Baiz et al., 2009; Zanetti et al., 2008).

2.4. QRT-PCR

Total RNA was extracted, quantified and the quality evaluated as reported (Biolo et al., 2006; Farra et al., 2011). Reverse transcription was performed using 1 μg of total RNA in the presence of random hexamers and MuLV reverse transcriptase (Applera Corporation, USA). The primers (Eurofins Genomics, 300 nM, Table 2) and the Real-Time amplification conditions for eEF1A1/eEF1A2 (Scaggiante et al., 2012), for E2F1/E2F2/E2F3/Cyclin E1 (Baiz et al., 2014), for 2′,5′-oligoadenylate synthetase 1 (OAS1) and for 28S RNA (Dapas et al., 2009), have been already described. The relative amounts of the target mRNA were normalized by 28S rRNA content.

Table 1
siRNA sequences.

siRNA	Sense	Antisense
siE2F1 rat	5-GAGGGCAUUAGAGAUCUCU-3	5-AGAGAUCUCUAAUGCCCUC-3
siE2F1 human	5-GAGGAGUUCAUCAGCCUUU-3	5-AAAGGCUGAUGAACUCCUC-3
siA1 human/rat	5-AUGCGGUGGCAUCGACAAA-3	5-UUUGUCGAUGCCACCGCAU-3
siA2 human/rat	5-GUCGGCUUCAAUGUGAAGA-3	5-UCUUCACAUUGAAGCCGAC-3
siA2bis human/rat	5-UCGAACUUCUCAAUGGUCC-3	5-GGACCAUUGAGAAGUUCGA-3
siGL2	5-CGUACGCGGAAUACUUCGA-3	5-UCGAAGUAUUCCGCGUACG-3

Table 2

RT-PCR primer sequences.

| Gene	Forward	Reverse
eEF1A1	5′-AAC ATT GTC GTC ATT GGA CA-3′	5′-ACT TGC TGG TCT CAA ATT TC-3′
eEF1A2	5′-GCC ACC GTC AAT AGG TGG AC-3′	5′-TGA TGT GGG TCT TCT CCT TG-3′
E2F1	5′-CCA GGA AAA GGT GTG AAA TC-3′	5′ AAG CGC TTG GTG GTG AGA TT-3′
E2F2	5′-CAA GTT GTG CGA TGC CTG C-3′	5′-TCC CAA TCC CCT CCA GAT C-3′
E2F3	5′-AAG TGC CTG ACT CAA TAG AGA GCC-3′	5′-AGT CTC TTC TGG ACA TAA GTA AAC CTC A-3′
Cyclin E1	5′-TGC CTG TAC TGA GCT GGG CA-3′	5′-GGC TGC AGA AGA GGG TGT TG-3′
Cyclin E1 rat	5′-GTG AAA AGC CAG GAT AGC AG-3′	5′-GAG GCT GAA ATG CAG TCT TG-3′
28S	5′- TGG GAA TGC AGC CCA AAG-3′	5′- CCT TAC GGT ACT TGT TGA CTA TGC-3′
OAS1	5-TCC AAG GTG GTA AAG GGT GG-3′	5′AGG TCA GCG TCA GAT CGG C-3′

2.5. Western blotting

Protein extraction was performed as described (Farra et al., 2011). Briefly, 30 μg of protein extract were resolved onto 12% SDS-PAGE and blotted onto a 0.22 μm nitrocellulose membrane (Schleicher & Schuell, Keene, NH). The rabbit monoclonal antibody anti-eEF1A1 (AbCam, Cambridge, UK, dilution 1:1000), the rabbit polyclonal antibody anti-eEF1A2 (Santa Cruz, CA, USA, dilution 1:1000) and the rabbit polyclonal antibody anti E2F1 (Santa Cruz, CA, USA, dilution 1:100) were used. In the same membrane, the loaded control protein GAPDH (Santa Cruz, CA, USA, dilution 1:1000) was probed. Blots were developed using the corresponding secondary horseradish peroxidase antibodies (Santa Cruz, CA, USA) by enhanced chemiluminescence detection system (Pierce,

Rockford, IL, USA) and exposed to Kodak film (Sigma-Aldrich, St. Louis, MO, USA). Particular care was taken to appropriately developing Kodak film in order to generate non-saturated bands. Band intensities were measured by densitomer (Model GS-700 Imaging Densitometer, Biorad) equipped with the Molecular analyst software (Biorad).

2.6. Over-expression of E2F1

The E2F1 expressing plasmid (pE2F1, a kind gift from Prof G. Del Sal, Dep. of Life Sciences, University of Trieste, Italy) drives E2F1 expression from a cytomegalovirus promoter as reported (Baker et al., 1990). Optimal transfection conditions were obtained by using Lipofectamine 2000 (1 mg/ml, Invitrogen) at a weight ratio
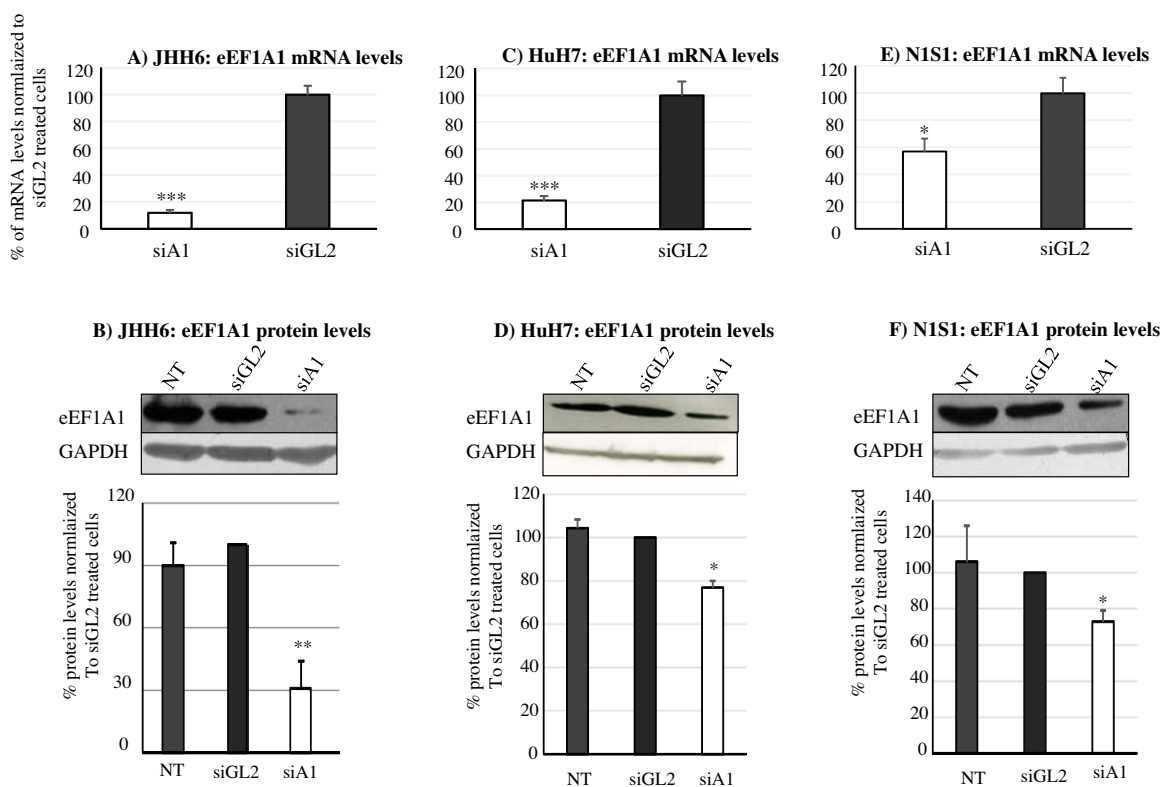
Fig. 1. siRNA effects on the mRNA and protein levels of eEF1A1.

A, C, E) Three days after transfection, the siRNA directed against eEF1A1 (siA1, 220 nM), significantly reduced the mRNA levels of the target in the cell lines tested compared to siRNA-control treated cells (siGL2, 220 nM). The data, normalized to 28S rRNA levels and expressed as the% of the average of the respective siGL2-treated cells, are shown as mean ± SEM; *** $p < 0.0003$ compared to control siGL2-treated cells; * $p < 0.02$ compared to control siGL2-treated cells; n = 6. B, D, F) Three days after transfection, the siRNA directed against eEF1A1 (siA1, 220 nM) significantly reduced the target protein levels in all cell lines tested compared to control treated cells (siGL2, 220 nM) and non-treated cells (NT). The data, normalized to GAPDH levels and expressed as% of the respective siGL2-treated cells, are shown as mean ± SEM; **$p < 0.0013$ compared to control siGL2-treated cells and NT; * $p < 0.038$ compared to control siGL2-treated cells and NT; n = 4.

plasmid/transfectant of 1:2.5 in HuH7. The mixture Liposome-plasmid (2 μg) was administered to 2.5×10^5 cells in 6 well plates for 4 h at 37 °C in Optimem medium. Thereafter, the medium was removed and the cells were overlaid with their specific growth medium. Based on our previous experience (Farra et al., 2015a) we know that on average, 79% of HuH7 can be transfected. As control plasmid, we used pEGFP-C1 (BD-Biosciences Clontech), which expresses the enhanced green fluorescence protein (EGFP) from a cytomegalovirus promoter. The day after the transfection with either pE2F1 or pEGFP, the cells were transfected with siA1 or siGL2; two days later, cells were collected and the number of cells and the mRNA levels of E2F1\eEF1A1, determined.

2.7. Statistical analysis

P values were calculated by the GraphPad InStat tools (Graph-Pad Software, Inc., La Jolla, CA, USA) using the unpaired *t*-test with or without Welch correction and the Mann-Whitney Test, Wilcoxon matched-pairs signed-ranks test, as appropriate. P values < 0.05 were considered statistically significant.

3. Results

3.1. siRNA effectiveness and specificity in depleting eEF1A1 and eEF1A2

As models of HCC, we have considered the human HCC cell lines HuH7 and JHH6 as they represent a different stage of tumor differentiation and thus phenotypic-related effects of eEF1A depletion can be studied (Grassi et al., 2007). Moreover, HuH7 (Venturelli et al., 2007) and JHH6 (Tonon et al., 2016) can be used in animal models of HCC. We also considered the rat HCC cell line N1S1, usable in a syngenic orthotopic rat model of HCC (Lee et al., 2014).

We verified that siRNA transfection efficiencies were similar among the different cell lines (Suppl. mat. 1), and that three days after siRNA transfection was the optimal analysis time to study siRNA silencing effects. Thus, most of the data reported in the present work refer to this time point.

While the siRNA targeting eEF1A1 (siA1) has been already described (Lamberti et al., 2007) the one targeting eEF1A2 (siA2) has been designed by us. In each cell line, siA1 significantly reduced the mRNA (Fig. 1A, C, E) and protein (Fig. 1B, D, F) levels of its target. Similarly did siA2 in HuH7 and JHH6 for the mRNA (Fig. 2A, C) and protein levels (Fig. 2B, D). Notably, a different siRNA against eEF1A2 gave comparable results in JHH6 (siA2bis, Suppl. mat. 2A, B). In N1S1, we could not amplify eEF1A2 mRNA probably due to mutation(s) in the primers binding regions; however, siA2 effects was proven at the protein level (Fig. 2E). Notably, siA1 and siA2 effects, cannot be ascribed to an unspecific induction of the interferon response (Sledz et al., 2003) as no relevant increase of OAS1 gene expression was observed (Suppl. mat 3). Moreover, we could prove the specificity of the effects of siA1 and siA2 on eEF1A2 and eEF1A1 protein levels, respectively (Suppl. mat 4). Indeed neither siA1 nor siA2 affected the levels of eEF1A2 or eEF1A1,
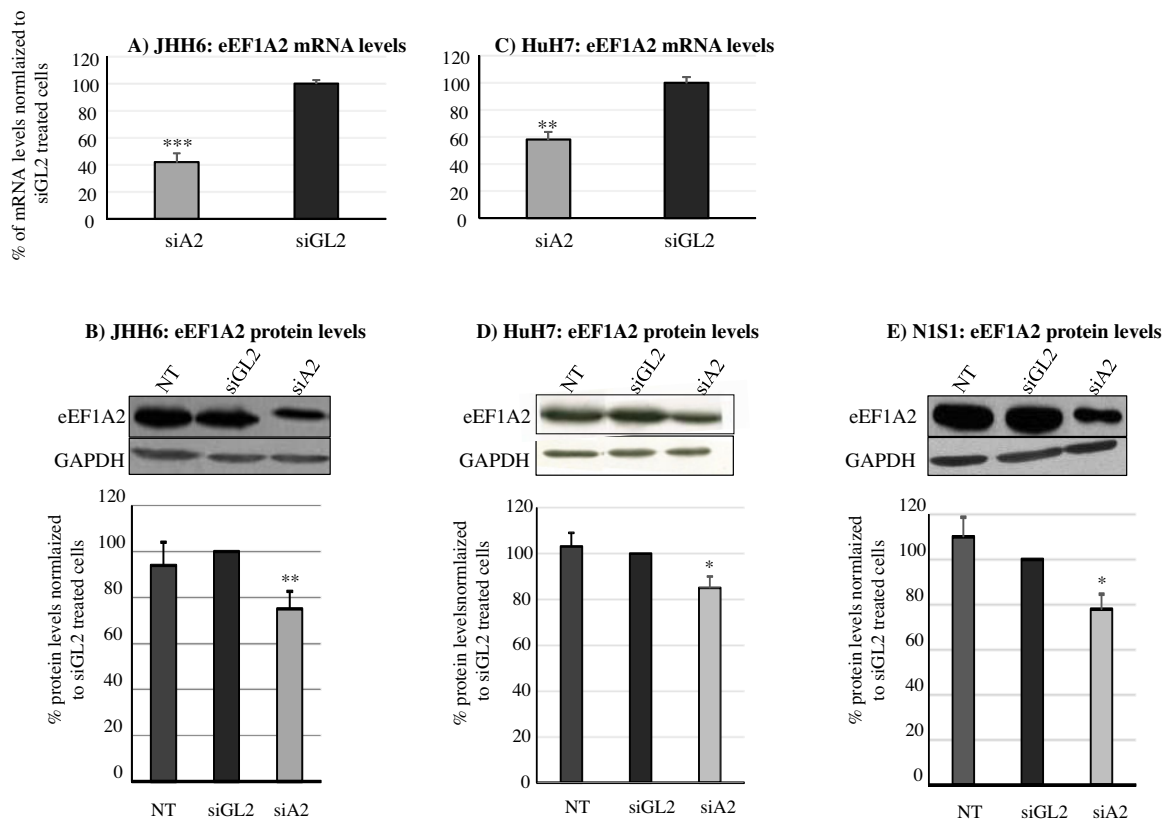
Fig. 2. siRNA effects on the mRNA and protein levels of eEF1A2.
A, C) Three days after transfection, the siRNA directed either against eEF1A2 (siA2, 220 nM), significantly reduced the mRNA levels of the target in the cell lines tested compared to siRNA-control treated cells (siGL2, 220 nM). The data, normalized to 28S rRNA levels and expressed as% of the average of the respective siGL2-treated cells, are shown as mean ± SEM; *** $p < 0.0001$ compared to control siGL2-treated cells; ** $p < 0.0021$ compared to control siGL2-treated cells, n = 6. B, D, E) Three days after transfection, the siRNA directed against eEF1A2 (siA2, 220 nM) significantly reduced the target protein levels in all cell lines tested compared to control treated cells (siGL2, 220 nM) and non-treated cells (NT). The data, normalized to GAPDH levels and expressed as the% of the respective siGL2-treated cells, are shown as mean ± SEM; ** $p < 0.01$ compared to control siGL2-treated cells and NT; * $p < 0.035$ compared to control siGL2-treated cells and NT; n = 4.
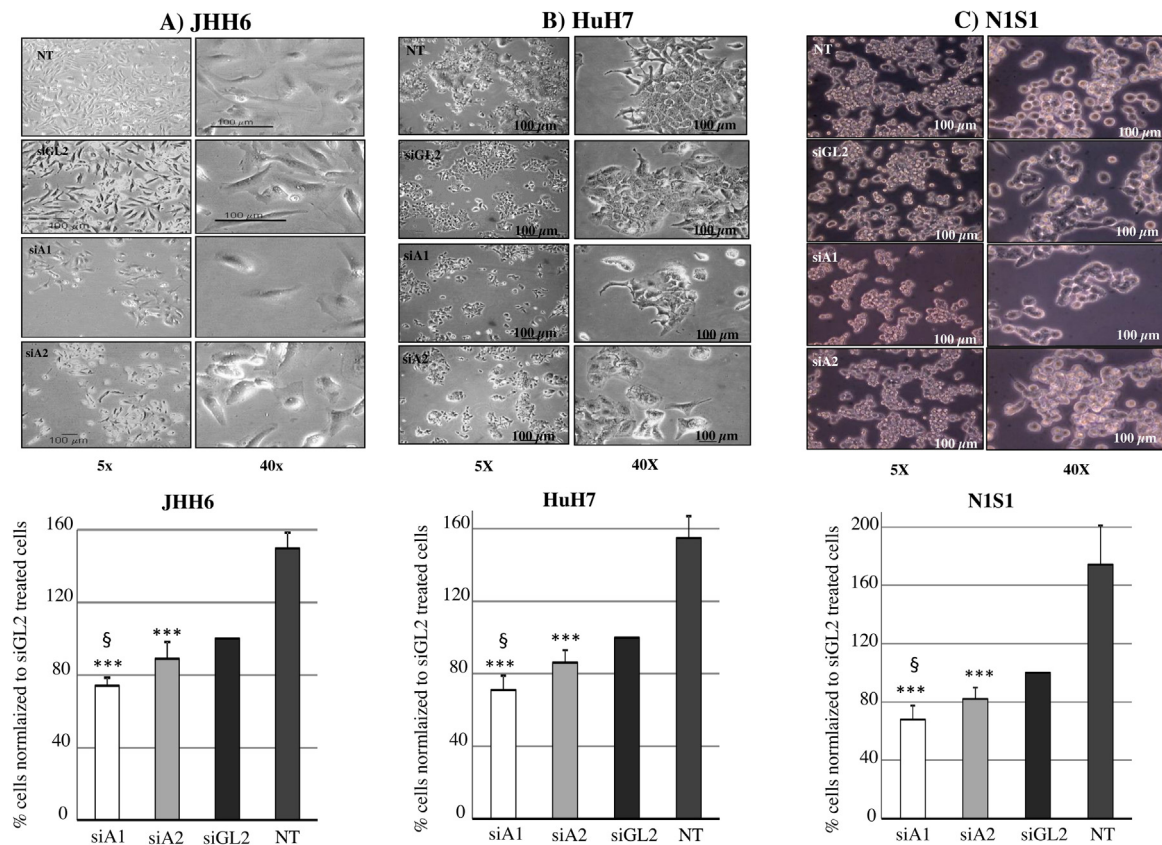
Fig. 3. siRNA effects on cell number.

A–C) Upper panels: three days after transfection, cell morphology was analyzed by phase contrast microscopy at 5× and 40× magnification, representative fields are shown; siA1 (siRNA against eEF1A1, 220 nM), siA2 (siRNA against eEF1A2, 220 nM), NT (non-treated cells), siGL2 (control siRNA against the luciferase mRNA, 220 nM). Lower panels: three days after transfection, siA1 or siA2 significantly reduced the cell number in all cell lines tested compared to siGL2-treated cells and NT. The data, expressed as the% of siGL2 treated cells, are shown as mean ± SEM; *** p < 0.001 compared to control siGL2-treated cells and NT. In all cell lines, the reduction in the amount of cells observed following eEF1A1 depletion was always superior to that induced by eEF1A2 depletion, § p < 0.049 compared to siA2-treated cells; n = 7.

respectively. This is a relevant requirement to investigate the independent contribution of eEF1A1 and eEF1A2 to HCC.

### 3.2. Phenotypic effects of eEF1A1 or eEF1A2 silencing

Three days following eEF1A1 or eEF1A2 depletion, a significant reduction in cell number as shown by microscopy inspection and cell counting (Fig. 3), was observed. This effect was always more evident following eEF1A1 than eEF1A2 depletion. In JHH6 and HuH7, eEF1A1 or eEF1A2 depletion also decreased cell viability (Fig. 4A, B and Suppl. mat. 2C for siA2bis). In line with the cell counting data, in JHH6 and HuH7 six and ten days after siRNA transfection, respectively, cell vitality reduction was more evident following eEF1A1 than eEF1A2 depletion. A tendency toward this behavior was detected in N1S1 (Fig. 4C). Beside this, the vitality test revealed that whereas in JHH6 and HuH7 siRNA effect was visible up to day ten, in N1S1 it lasted up to day six following transfection.

We then explored the mechanism responsible for the reduction of cell number/viability following eEF1A1 or eEF1A2 depletion. As we could exclude significant effects promoting cell necrosis (Suppl. mat 5) and cell apoptosis (Suppl. mat 6), we concentrated the attention on cell cycle progression. In JHH6 and HuH7, both eEF1A1 and eEF1A2 depletion induced a significant increase of G1-G0 and a decrease of S phase cells (Fig. 4D, E). In N1S1, this was confirmed for eEF1A1 depletion while for eEF1A2 depletion we just observed a tendency towards this trend (Fig. 4F). Notably in all cell lines, the

increase of G1-G0 phase cells was always more evident following eEF1A1 than eEF1A2 silencing (Fig. 4D–F).

3.3. G1-G0 accumulation following eEF1A1 depletion involves E2F1 down-regulation

The G1 block induced by eEF1A1 or eEF1A2 depletion, prompted us to investigate the molecular mechanisms responsible for this observation. Based on our previous experience with G1 block in HCC (Farra et al., 2015a, 2010, 2011), we focused our attention on the possible role of E2F1. This is a transcription factor able to promote the G1 to S phase transition both in normal cells and in many tumor cells including HCC cells (Farra et al., 2017). In the cell lines considered, eEF1A1 (Fig. 5A–F) but not eEF1A2 depletion (data not shown) invariably resulted in the decrease of both mRNA and protein levels of E2F1, indicating the association between E2F1 expression down-regulation and the G1 block induced by eEF1A1 depletion. Notably, E2F1 depletion is *per se* responsible for a strong impairment of the vitality of JHH6/HuH7 (Farra et al., 2011) and N1S1 (Suppl. mat 7). Moreover, we observed that the decrease of E2F1 following eEF1A1 depletion, was paralleled by the contemporary reduction of the mRNA levels of different E2F1 transcriptional targets, *i.e.* E2F2, E2F3 and cyclin E1 (Fig. 5B, D, F). Being all these genes involved in the G1 to S phase transition (Bracken et al., 2004), this observation further contributes to explain the G1 block detected in the HCC cell lines considered. Finally, whereas eEF1A1 depletion affected E2F1
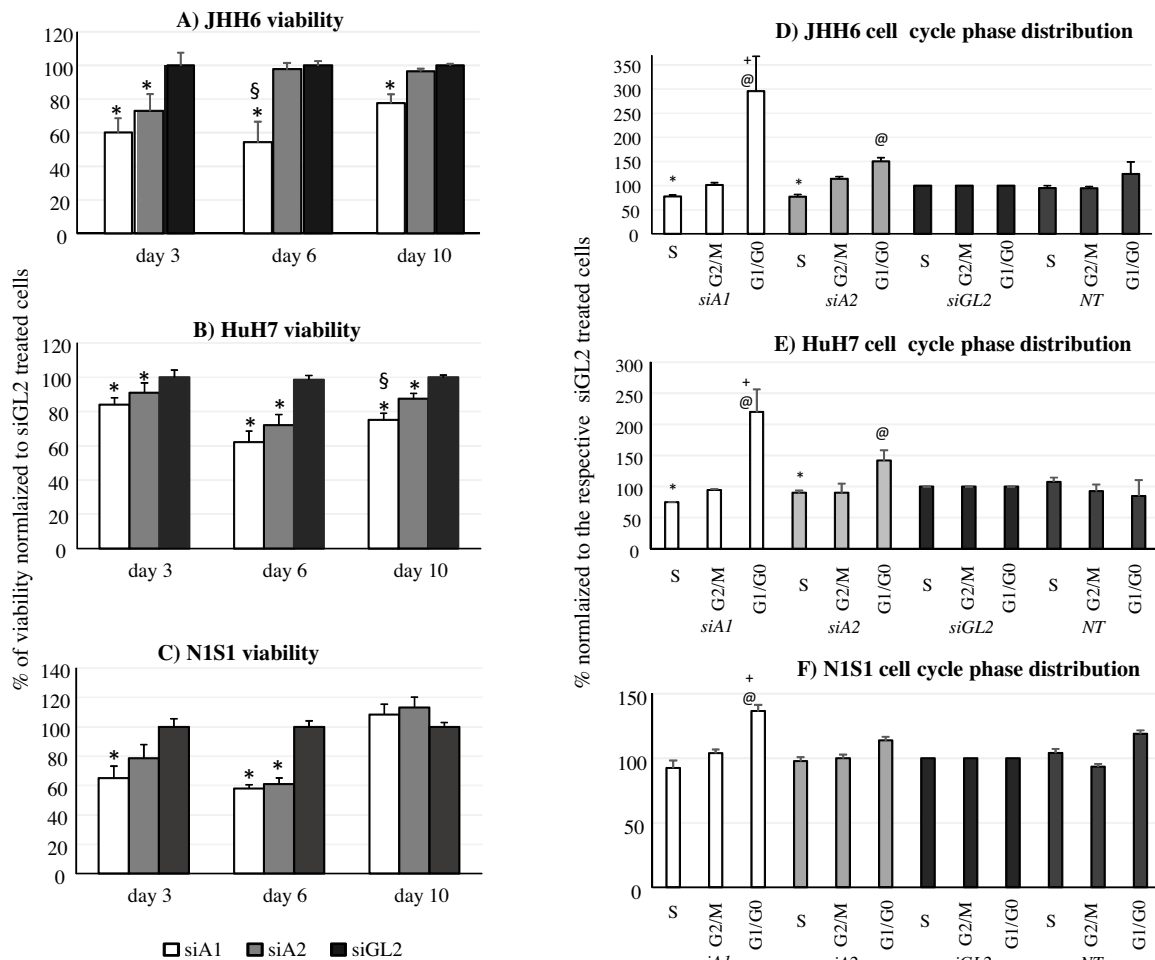
Fig. 4. siRNA effects on cell viability and cell cycle phase distribution.

A–C) siRNAs directed against either eEF1A1 (siA1, 220 nM) or eEF1A2 (siA2, 220 nM) were delivered to 96-well-plate cultured cells; the effects on cell viability were evaluated by MTT test at different times following delivery in comparison to siGL2 (control siRNA against the luciferase mRNA, 220 nM) treated cells. The data, expressed as% of the average of cells treated by siGL2, are shown as mean ± SEM, n = 9;. * p < 0.04, compared to siGL2, § p < 0.025 compared to siA2. D–F) The effects of siA1 (220 nM) and siA2 (220 nM) on cell cycle phase distribution were evaluated three days after siRNA delivery. The data for each cell cycle phase are reported as the% of the values of the respective cell cycle phase of siGL2 treated; data are shown as mean ± SEM, n = 5. * p < 0.019 compared to the S phase of the control siGL2-treated and NT (non-treated cells), @ p < 0.028 compared to the G1\G0 phase of the control siGL2-treated and NT, + p < 0.028 compared to siA2 G1\G0 phase.

expression levels, the opposite was not true. Indeed, E2F1 depletion by a specific siRNA (Farra et al., 2011), did not significantly alter eEF1A1 protein levels (Suppl. mat 8) suggesting a univocal relation eEF1A1 *vs* E2F1.

To conclusively proving the functional involvement of E2F1 down-regulation in the G1 block induced by eEF1A1 depletion, we studied whether E2F1 overexpression (plasmid pE2F1) could attenuate the block of cell proliferation induced by eEF1A1 depletion (siA1). For this test, we used the HuH7 cell line due to the increased resistance to the combined transfection procedure (pE2F1 + siA1) with respect to the other two cell lines. Compared to control (pE2F1 + siGL2 transfected cells), pE2F1 + siA1 transfected cells displayed a significant reduction of eEF1A1 but not of E2F1 mRNA levels (Fig. 6A) that, in contrast, we observed just after eEF1A1 depletion (Fig. 5). The lack of E2F1 down-regulation resulted in no evident reduction in cell proliferation as evaluated by cell counting (Fig. 6B). We then explored the effects of the overexpression of the irrelevant gene EGFP (pEGFP) still maintaining eEF1A1 depletion (siA1). Under these conditions, we observed a reduction of both eEF1A1 and E2F1 mRNA levels (Fig. 6C) compared to control (pEGFP + siGL2 transfected cells). In parallel, a decrease of cell growth was observed in pEGF + siA1 treated cells (Fig. 6D) compared to control (pEGFP + siGL2

transfected cells). Thus, the overexpression of E2F1, but not that of an irrelevant gene, can attenuate the proliferation block induced by eEF1A1 depletion. This strongly support the functional role of E2F1 down-regulation in the growth arrest promoted by eEF1A1 depletion.

4. Discussion

Despite the evidences of the involvement of eEF1A1 and eEF1A2 in HCC, the quantitative contribution of each of the two isoforms to the disease is not yet clear. Here we desired to determine if one of the two isoform is more involved in HCC than the other one or both contribute equally to the disease.

The two isoforms have been independently depleted putting particular care to use siRNAs able to selectively targeting each isoform without affecting the other one. This is not a trivial aspect due to the high sequence homology between eEF1A1 and eEF1A2 (Lund et al., 1996). Being this prerequisite satisfied by our siRNAs (Suppl. mat 4), the reliability of the data obtained is ensured. Moreover, as none of the siRNAs used significantly triggered OAS1 (Suppl. mat 3), we can exclude any unspecific effects due to the induction of the interferon response (Sledz et al., 2003) which could have influenced the results. Finally, as the siRNA transfection
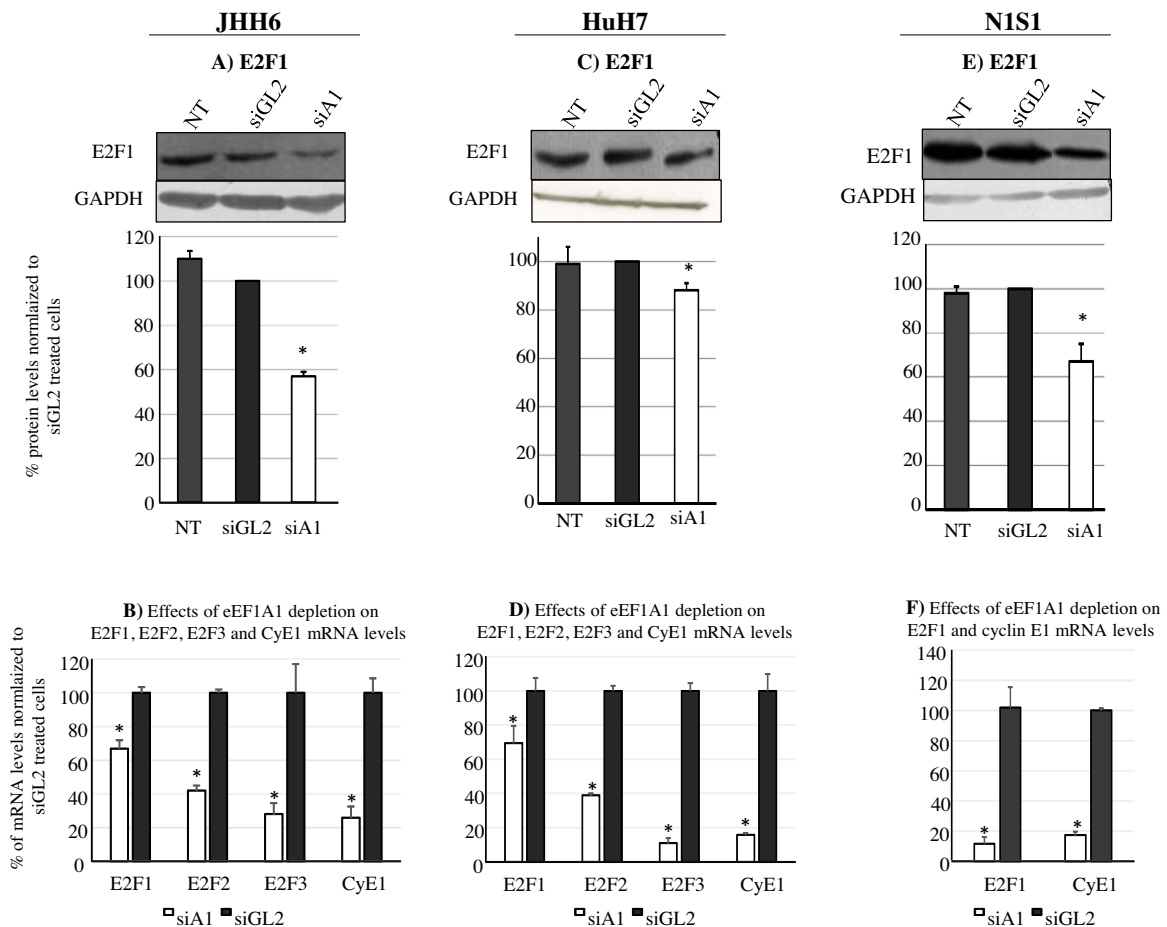
Fig. 5. Effects of eEF1A depletion on E2F1 and related target transcripts.

A,C,E) Three days after eEF1A1 silencing by siRNA (siA1, 220 nM), the protein level of E2F1 were evaluated. The representative blots shown belong to the same experiments reported in Fig. 1 B,D,F. In all cell lines, eEF1A1 depletion was paralleled by a decrease of E2F1 protein levels compared to control treated cells (siGL2, 220 nM) and non-treated cells (NT). The data, normalized to GAPDH levels and to the siGL2-treated cells, are shown as mean ± SEM, n = 4. *p < 0.035 compared to control siGL2-treated cells and NT. B,D, F) Three days after eEF1A1 silencing by siRNA (siA1, 220 nM), the mRNA levels of E2F1 and of related transcripts (E2F2, E2F3, cyclin E1) were evaluated. The data, normalized to 28S rRNA levels and expressed as the% of the average of the respective siGL2-treated cells, are shown as mean ± SEM, n = 6; * p < 0.034 compared to the respective control siGL2-treated cells.

efficiencies were similar in all the different cell lines used (Suppl. mat 1), the comparison of the effects of either eEF1A1 or eEF1A2 depletion among the cell lines is feasible.

Our data indicate that both eEF1A1 and eEF1A2 depletion (Figs. 1 and 2) resulted in an impairment of cell vitality and growth (Figs. 3 and 4). Notably, however, the effects of eEF1A1 depletion were always superior to those of eEF1A2 as indicated by cell counting (Fig. 3) and by viability tests in HuH7 and N1S1 (Fig. 4B–C). In particular, we observed that eEF1A1 depletion induced a more pronounced arrest of the cells in the G1 phase of the cell cycle compared to eEF1A2 depletion (Fig. 4E–F). Together these data indicate that both eEF1A1 and eEF1A2 contribute to HCC cells proliferation; however, eEF1A1 seems to have a preponderant role over eEF1A2 in the HCC cell lines considered HCC.

In JHH6, eEF1A1 depletion also resulted in an increased reduction of cell growth compared to eEF1A2 depletion (Figs. 3 A, Fig. 4A and D). However, in JHH6 the extent of eEF1A1 depletion was superior to that of eEF1A2 (compare Fig. 1B with Fig. 2B). This opens the possibility that in JHH6 the increased effect of eEF1A1 depletion may depend on a more pronounced decrease of eEF1A1 protein. However, we believe this may not necessarily impair the comparison between the phenotypic effects of siA1 and with siA2. By looking at the eEF1A1 protein level and the cell number of each single experiment performed in JHH6 (Suppl. mat 9), it results that

below a certain eEF1A1 threshold (down to about 70%), the number of cell does not further decrease. This suggests that even if siA1 is more effective in reducing eEF1A1 compared to siA2, the comparison of the effects at the cell count level is feasible. This interpretation can also explain the fact that whereas in HuH7/N1S1 siA1 reduces the eEF1A1 protein level down to about 80%, the consequent reduction in cell number (Fig. 3) is comparable to that observed in JHH6, where eEF1A1 reduction is more pronounced (down to 30%). Thus, whereas further studies in vitro and in animal models of HCC (Lee et al., 2014; Tonon et al., 2016; Venturelli et al., 2007) are necessary, it is unlikely that the more pronounced reduction of eEF1A1 compared to eEF1A2 in JHH6, prevents the comparison of the effects at the phenotypic level.

The cell cycle impairment induced by eEF1A depletion is in agreement with previous works dealing with eEF1A and HCC (Elgohary et al., 2015; Pellegrino et al., 2014; Qiu et al., 2016; Schlaeger et al., 2008). Notably, however, the targeting of eEF1A by a DNA aptamer we previously performed (Scaggiante et al., 2016) did not result in a significant impairment of the cell cycle, still inducing a prominent reduction in cell vitality. The reason for this apparent discrepancy may depend on the use of either siRNAs or aptamers as targeting molecules. Whereas the siRNA-based approach represses the synthesis of eEF1A, reducing both the cytoplasmic (more involved in protein synthesis) and the

A) eEF1A1 and E2F1 mRNA levels

B) Cell counting

C) eEF1A1 and E2F1 mRNA levels

D) Cell counting
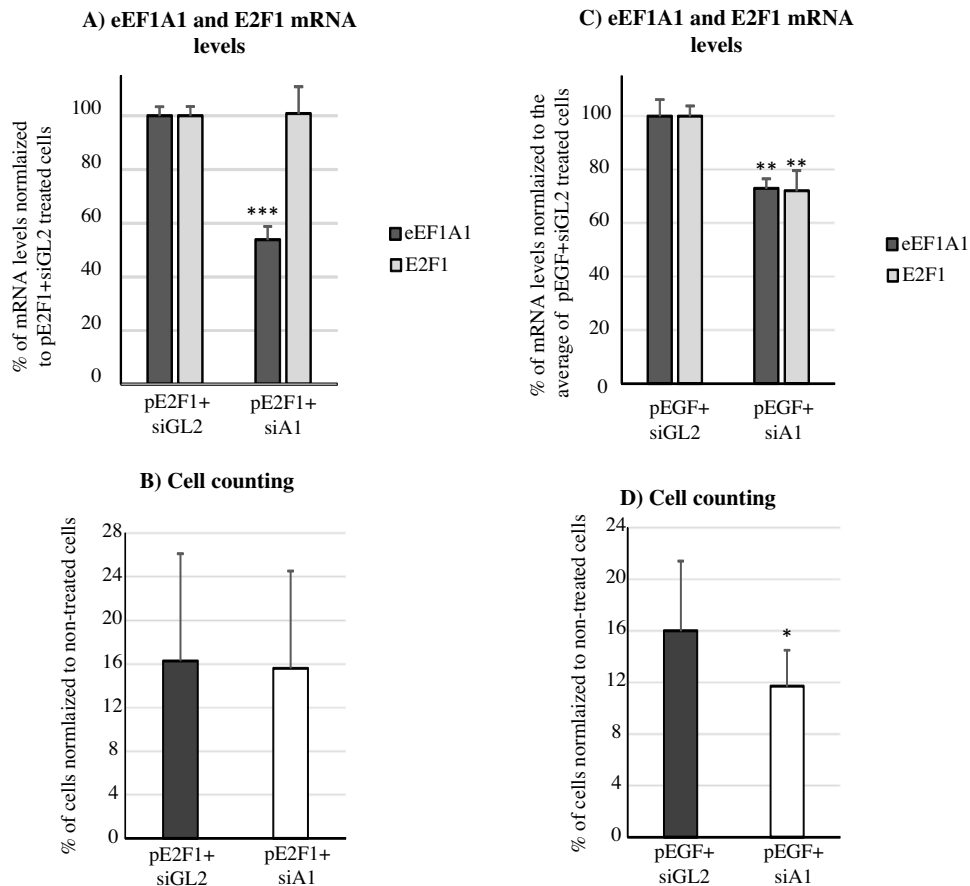
Fig. 6. Effects of E2F1 overexpression and eEF1A1 depletion in HuH7.
A,C) Three days after pE2F1/pEGFP and siA1/siGL2 transfection in HuH7, the mRNA levels of eEF1A1 and E2F1 were evaluated (pE2F1 = plasmid overexpressing E2F1; pEGFP = plasmid overexpressing enhanced green fluorescence protein; siA1 = siRNA against eEF1A1; siGL2 = control siRNA against luciferase mRNA). The data, normalized to 28S rRNA levels and expressed as the average of the respective siGL2-treated cells (pE2F1 + siGL2 or pEGFP + siGL2), are shown as mean ± SEM, n = 6. *** p < 0.0001 compared to control pE2F1 + siGL2-treated cells; ** p < 0.0034 compared to control pEGF + siGL2-treated cells. B,D) Three days after pE2F1/pEGFP and siA1/siGL2 transfection in HuH7, cell number was evaluated. The data, normalized to non-treated cells (NT), are expressed as mean ± SEM, n = 4; * p < 0.03 compared to control pEGF + siGL2-treated cells

cytoskeletal-nuclear fractions (more involved in the non-canonical functions) of eEF1A, the aptameric-based approach mainly interacts with the cytoskeletal/nuclear fraction (Dapas et al., 2003; Scaggiante et al., 2006). It is thus conceivable that the targeting of different sub cellular fractions of the eEF1A protein can result in divergent phenotypic effects.

In JHH6 and HuH7, eEF1A1 and eEF1A2 depletion impaired cell vitality up to ten days post transfection (Fig. 4A–B) almost doubling the effects induced by E2F1 silencing we previously observed (Farra et al., 2011). This suggests that eEF1A rather than E2F1 may be a preferred target to obtain a more durable suppression of HCC cell growth. In N1S1, eEF1A1/eEF1A2 depletion impaired cell vitality up to six instead of ten days post transfection (Fig. 4C). Whereas the reasons for this observation deserve further investigation, it is possible that the faster proliferation rate of N1S1 compared to JHH6/HuH7, contributes to the faster "dilution" of the siA1/siA2 in the cytoplasm following cell division. This in turn reduces the extent of the effects on cell viability in the daughter cells. Despite this, our data confirm and extend to a rat HCC cell line the effectiveness of eEF1A targeting to down modulate HCC cell growth.

In cell counting (Fig. 3) and cell cycle experiments (Fig. 4D, E), the more pronounced effect of eEF1A1 over eEF1A2 depletion is observed already three days post transfection. However, in cell vitality tests, this effect occurs at later time points (day six for JHH6 and day ten for HuH7 (Fig. 4A–B)). We believe this depends on the fact that while the vitality tests have been performed in 96 well

plates, the cell counting and cell cycle experiments have been performed in 6 well plates (to have an appropriate amount of cell for counting and performing cell cycle analysis). In line with our previous experience (Farra et al., 2011), cell cultured in 96 wells require longer time to recover from transfection most likely because of the more unfavorable culturing conditions (reduced cell number and medium) compared to 6 well culturing. We believe this aspect can contribute to explain the delay in the appearance of the difference between eEF1A1 and eEF1A2 silencing in viability tests.

The siRNA-mediated depletion of eEF1A1 and eEF1A2 results in a G1 block of the cells (Fig. 4D–F). Interestingly, only for eEF1A1 this depends on the depletion of E2F1 (Figs. 5 and 6). Thus, for the first time, we report the functional relation between eEF1A1 and E2F1 in HCC cell lines. Indeed, we show that eEF1A1 depletion is paralleled by E2F1 decrease (Fig. 5A–F) and that E2F1 over expression can attenuate the cell growth inhibition induced by eEF1A1 depletion (Fig. 6). eEF1A2 depletion, which does not induce E2F1 down-regulation (data not shown), most likely causes the G1 accumulation by impairing the PI3K/Akt/NF-κB pathway (Qiu et al., 2016) and/or inactivating p53 via PI3K/AKT/mTOR-dependent stabilization of MDM4 (Pellegrino et al., 2014) as previously reported. The different mechanism of action here observed for eEF1A1 and eEF1A2 is in line with the knowledge that the two isoforms, despite being very similar, can differ in the biological effects triggered with regard to their non-canonical functions (Scaggiante et al., 2014).

The fact that eEF1A1 depletion decreases E2F1 but non vice-versa (Suppl. mat 8), suggests a unidirectional relation between eEF1A1 and E2F1. However, how can eEF1A1 affect E2F1 mRNA and protein levels? A possibility is that the impairment of eEF1A1 reduces E2F1 translation thus reducing E2F1 protein levels. This in turn reduces E2F1 transcript levels as E2F1 promotes its own transcription (Attwooll et al., 2004). Interestingly, the ability of eEF1A1 to regulate the expression of a specific protein has been recently shown for the heat shock protein 70 (HSP70)(Vera et al., 2014). In this case, eEF1A1 regulates HSP70 induction from transcription activation to mRNA stabilization, nuclear transport, and translation control. Whether eEF1A1 controls E2F1 expression via similar mechanisms remains to be determined.

The impairment of E2F1 transcriptional activity following eEF1A1 depletion, is also witnessed by the reduction of the mRNA levels of different E2F1 known transcripts such as E2F2, E2F3 and cyclin E1 (Fig. 5 B,D,F). Moreover, the decreased expression of these genes, all involved in the G1 to S phase transition (Bracken et al., 2004), further justifies the G1 block observed.

As above discussed, both eEF1A isoforms are potentially suitable targets to hit for HCC cell growth inhibition. However, our data indicate that eEF1A1 rather than eEF1A2 targeting is more effective. The choice of eEF1A1 as preferred target implies the development of a targeted delivery system able to discriminate between normal hepatocytes and tumor cells. Indeed, eEF1A1 is expressed in both normal and HCC cells. Thus, the indiscriminate depletion of eEF1A1 may affect normal hepatocytes. This problem may be not present using eEF1A2 as target since it is not expressed in normal hepatocytes. Nevertheless, it should be avoided eEF1A2 depletion in tissues (nervous system, muscle) physiologically expressing it. Thus, for systemic administration, also eEF1A2 targeting requires a HCC specific delivery approach. In this regard, the development of HCC targeted delivery systems is under active investigation by different groups including our group (Cavallaro et al., 2014; Farra et al., 2015b; Posocco et al., 2015; Sardo et al., 2015).

In conclusion, we show that the independent targeting of the two eEF1A isoforms is effective in reducing HCC cell growth. Moreover, our data open the possibility that eEF1A1 rather than eEF1A2 depletion results in a more effective down regulation of HCC cell growth. Finally, we provide evidences that the growth arrest induced by eEF1A1 depletion depends on the down regulation of E2F1, a transcription factor known to be involved in HCC development and maintenance.

Acknowledgements

References

Abbas, W., Kumar, A., Herbein, G., 2015. The eEF1A proteins: at the crossroads of oncogenesis, apoptosis, and viral infections. Front. Oncol. 5, 75.

Attwooll, C., Lazzerini, D.E., Helin, K., 2004. The E2F family: specific functions and overlapping interests. EMBO J. 23, 4709–4716.

Azmi, A.N., Chan, W.K., Goh, K.L., 2015. Sustained complete remission of advanced hepatocellular carcinoma with sorafenib therapy. J. Dig. Dis..

Baiz, D., Pozzato, G., Dapas, B., Farra, R., Scaggiante, B., Grassi, M., Uxa, L., Giansante, C., Zennaro, C., Guarnieri, G., Grassi, G., 2009. Bortezomib arrests the proliferation of hepatocellular carcinoma cells HepG2 and JHH6 by differentially affecting E2F1, p21 and p27 levels. Biochimie 91, 373–382.

Baiz, D., Dapas, B., Farra, R., Scaggiante, B., Pozzato, G., Zanconati, F., Fiotti, N., Consoloni, L., Chiaretti, S., Grassi, G., 2014. Bortezomib effect on E2F and cyclin family members in human hepatocellular carcinoma cell lines. World J. Gastroenterol. 20, 795–803.

Baker, S.J., Markowitz, S., Fearon, E.R., Willson, J.K., Vogelstein, B., 1990. Suppression of human colorectal carcinoma cell growth by wild-type p53. Science 249, 912–915.

Biolo, G., Amoroso, A., Savoldi, S., Bosutti, A., Martone, M., Pirulli, D., Bianco, F., Ulivi, S., Bertok, S., Artero, M., Barazzoni, R., Zanetti, M., Grassi, G., Guarnieri, G., Panzetta, G., 2006. Association of interferon-gamma +874A polymorphism with reduced long-term inflammatory response in haemodialysis patients. Nephrol. Dial. Transplant. 21, 1317–1322.

Bracken, A.P., Ciro, M., Cocito, A., Helin, K., 2004. E2F target genes: unraveling the biology. Trends Biochem. Sci. 29, 409–417.

Cavallaro, G., Licciardi, M., Amato, G., Sardo, C., Giammona, G., Farra, R., Dapas, B., Grassi, M., Grassi, G., 2014. Synthesis and characterization of polyaspartamide copolymers obtained by ATRP for nucleic acid delivery. Int. J. Pharm. 466, 246–257.

Dapas, B., Tell, G., Scaloni, A., Pines, A., Ferrara, L., Quadrifoglio, F., Scaggiante, B., 2003. Identification of different isoforms of eEF1A in the nuclear fraction of human T-lymphoblastic cancer cell line specifically binding to aptameric cytotoxic GT oligomers. Eur. J. Biochem. 270, 3251–3262.

Dapas, B., Farra, R., Grassi, M., Giansante, C., Fiotti, N., Uxa, L., Rainaldi, G., Mercatanti, A., Colombatti, A., Spessotto, P., Lacovich, V., Guarnieri, G., Grassi, G., 2009. Role of E2F1-cyclin E1-cyclin E2 circuit in human coronary smooth muscle cell proliferation and therapeutic potential of its downregulation by siRNAs. Mol. Med. 15, 297–306.

Elgohary, N., Pellegrino, R., Neumann, O., Elzawahry, H.M., Saber, M.M., Zeeneldin, A.A., Geffers, R., Ehemann, V., Schemmer, P., Schirmacher, P., Longerich, T., 2015. Protumorigenic role of Timeless in hepatocellular carcinoma. Int. J. Oncol. 46, 597–606.

Farra, R., Dapas, B., Pozzato, G., Giansante, C., Heidenreich, O., Uxa, L., Zennaro, C., Guarnieri, G., Grassi, G., 2010. Serum response factor depletion affects the proliferation of the hepatocellular carcinoma cells HepG2 and JHH6. Biochimie 92, 455–463.

Farra, R., Dapas, B., Pozzato, G., Scaggiante, B., Agostini, F., Zennaro, C., Grassi, M., Rosso, N., Giansante, C., Fiotti, N., Grassi, G., 2011. Effects of E2F1-cyclin E1-E2 circuit down regulation in hepatocellular carcinoma cells. Dig. Liver Dis. 43, 1006–1014.

Farra, R., Dapas, B., Baiz, D., Tonon, F., Chiaretti, S., Del, S.G., Rustighi, A., Elvassore, N., Pozzato, G., Grassi, M., Grassi, G., 2015a. Impairment of the Pin1/E2F1 axis in the anti-proliferative effect of bortezomib in hepatocellular carcinoma cells. Biochimie 112, 85–95.

Farra, R., Grassi, M., Grassi, G., Dapas, B., 2015b. Therapeutic potential of small interfering RNAs/micro interfering RNA in hepatocellular carcinoma. World J. Gastroenterol. 21, 8994–9001.

Farra, R., Grassi, G., Tonon, F., Abrami, M., Grassi, M., Pozzato, G., Fiotti, N., Forte, G., Dapas, B., 2017. The role of the transcription factor E2F1 in hepatocellular carcinoma. Curr. Drug Deliv. (in press).

Ferlay, J., Soerjomataram, I., Dikshit, R., Eser, S., Mathers, C., Rebelo, M., Parkin, D.M., Forman, D., Bray, F., 2015. Cancer incidence and mortality worldwide: sources, methods and major patterns in GLOBOCAN 2012. Int. J. Cancer 136, E359–E386.

Grassi, G., Schneider, A., Engel, S., Racchi, G., Kandolf, R., Kuhn, A., 2005. Hammerhead ribozymes targeted against cyclin E and E2F1 cooperate to down-regulate coronary smooth muscle cell proliferation. J. Gene Med. 7, 1223–1234.

Grassi, G., Scaggiante, B., Farra, R., Dapas, B., Agostini, F., Baiz, D., Rosso, N., Tiribelli, C., 2007. The expression levels of the translational factors eEF1A 1/2 correlate with cell growth but not apoptosis in hepatocellular carcinoma cell lines with different differentiation grade. Biochimie 89, 1544–1552.

Jemal, A., Bray, F., Center, M.M., Ferlay, J., Ward, E., Forman, D., 2011. Global cancer statistics. CA Cancer J. Clin. 61, 69–90.

Lamberti, A., Caraglia, M., Longo, O., Marra, M., Abbruzzese, A., Arcari, P., 2004. The translation elongation factor 1A in tumorigenesis, signal transduction and apoptosis: review article. Amino Acids 26, 443–448.

Lamberti, A., Longo, O., Marra, M., Tagliaferri, P., Bismuto, E., Fiengo, A., Viscomi, C., Budillon, A., Rapp, U.R., Wang, E., Venuta, S., Abbruzzese, A., Arcari, P., Caraglia, M., 2007. C-Raf antagonizes apoptosis induced by IFN-alpha in human lung cancer cells by phosphorylation and increase of the intracellular content of elongation factor 1A. Cell Death Differ. 14, 952–962.

Lee, T.K., Na, K.S., Kim, J., Jeong, H.J., 2014. Establishment of animal models with orthotopic hepatocellular carcinoma. Nucl. Med. Mol. Imaging 48, 173–179.

Lund, A., Knudsen, S.M., Vissing, H., Clark, B., Tommerup, N., 1996. Assignment of human elongation factor 1alpha genes: EEF1A maps to chromosome 6q14 and EEF1A2 to 20q13.3. Genomics 36, 359–361.

Pellegrino, R., Calvisi, D.F., Neumann, O., Kolluru, V., Wesely, J., Chen, X., Wang, C., Wuestefeld, T., Ladu, S., Elgohary, N., Bermejo, J.L., Radlwimmer, B., Zornig, M., Zender, L., Dombrowski, F., Evert, M., Schirmacher, P., Longerich, T., 2014. EEF1A2

inactivates p53 by way of PI3K/AKT/mTOR-dependent stabilization of MDM4 in hepatocellular carcinoma. Hepatology 59, 1886–1899.

Posocco, B., Dreussi, E., de Santa, J., Toffoli, G., Abrami, M., Musiani, F., Grassi, M., Farra, R., Tonon, F., Grassi, G., Dapas, B., 2015. Polysaccharides for the delivery of antitumor drugs. Materials 8, 2569–2615.

Qiu, F.N., Huang, Y., Chen, D.Y., Li, F., Wu, Y.A., Wu, W.B., Huang, X.L., 2016. Eukaryotic elongation factor-1alpha 2 knockdown inhibits hepatocarcinogenesis by suppressing PI3K/Akt/NF-kappaB signaling. World J. Gastroenterol. 22, 4226–4237.

Sardo, C., Farra, R., Licciardi, M., Dapas, B., Scialabba, C., Giammona, G., Grassi, M., Grassi, G., Cavallaro, G., 2015. Development of a simple, biocompatible and cost-effective inulin-diethylenetriamine based siRNA delivery system. Eur. J. Pharm. Sci. 75 (July (30)), 60–71.

Scaggiante, B., Dapas, B., Grassi, G., Manzini, G., 2006. Interaction of G-rich GT oligonucleotides with nuclear-associated eEF1A is correlated with their antiproliferative effect in haematopoietic human cancer cell lines. FEBS J. 273, 1350–1361.

Scaggiante, B., Dapas, B., Bonin, S., Grassi, M., Zennaro, C., Farra, R., Cristiano, L., Siracusano, S., Zanconati, F., Giansante, C., Grassi, G., 2012. Dissecting the expression of EEF1A1/2 genes in human prostate cancer cells: the potential of EEF1A2 as a hallmark for prostate transformation and progression. Br. J. Cancer 106, 166–173.

Scaggiante, B., Dapas, B., Farra, R., Tonon, F., Abrami, M., Grassi, M., Musiani, F., Zanconati, F., Pozzato, G., Grassi, G., 2014. In: Parsyan, A. (Ed.), Translation Elongation. Springer, pp. 241–265.

Scaggiante, B., Farra, R., Dapas, B., Baj, G., Pozzato, G., Grassi, M., Zanconati, F., Grassi, G., 2016. Aptamer targeting of the elongation factor 1A impairs

hepatocarcinoma cells viability and potentiates bortezomib and idarubicin effects. Int. J. Pharm. 506, 268–279.

Schlaeger, C., Longerich, T., Schiller, C., Bewerunge, P., Mehrabi, A., Toedt, G., Kleeff, J., Ehemann, V., Eils, R., Lichter, P., Schirmacher, P., Radlwimmer, B., 2008. Etiology-dependent molecular mechanisms in human hepatocarcinogenesis. Hepatology 47, 511–520.

Sledz, C.A., Holko, M., de Veer, M.J., Silverman, R.H., Williams, B.R., 2003. Activation of the interferon system by short-interfering RNAs. Nat. Cell Biol. 5, 834–839.

Tonon, F., Zennaro, C., Dapas, B., Carraro, M., Mariotti, M., Grassi, G., 2016. Rapid and cost-effective xenograft hepatocellular carcinoma model in Zebrafish for drug testing. Int. J. Pharm. 515, 583–591.

Venturelli, S., Armeanu, S., Pathil, A., Hsieh, C.J., Weiss, T.S., Vonthein, R., Wehrmann, M., Gregor, M., Lauer, U.M., Bitzer, M., 2007. Epigenetic combination therapy as a tumor-selective treatment approach for hepatocellular carcinoma. Cancer 109, 2132–2141.

Vera, M., Pani, B., Griffiths, L.A., Muchardt, C., Abbott, C.M., Singer, R.H., Nudler, E., 2014. The translation elongation factor eEF1A1 couples transcription to translation during heat shock response. Elife 3, e03164.

Yu, X., Liu, X., Liu, T., Hong, K., Lei, J., Yuan, R., Shao, J., 2012. Identification of a novel binding protein of FAT10: eukaryotic translation elongation factor 1A1. Dig. Dis. Sci. 57, 2347–2354.

Zanetti, M., Stocca, A., Dapas, B., Farra, R., Uxa, L., Bosutti, A., Barazzoni, R., Bossi, F., Giansante, C., Tedesco, F., Cattin, L., Guarnieri, G., Grassi, G., 2008. Inhibitory effects of fenofibrate on apoptosis and cell proliferation in human endothelial cells in high glucose. J. Mol. Med. 86, 185–195.